

Article

Low-Cost Alternative for Online Analysis of Volatile Organic Compounds

Benjamin Rico, Jon S. Sauer, Kimberly A. Prather,* and Robert S. Pomeroy



Cite This: Anal. Chem. 2024, 96, 10543-10550



Read Online

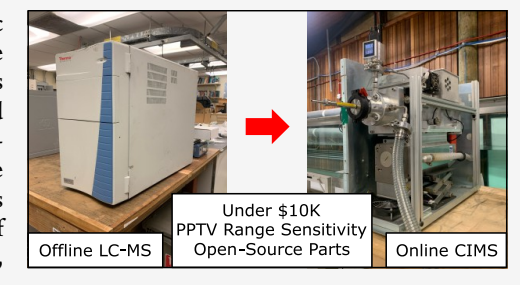
ACCESS I

Metrics & More

Article Recommendations

Supporting Information

ABSTRACT: The use of online mass spectrometry for detecting volatile organic compounds (VOCs) has proven to be a powerful technique, allowing for real-time analysis of many chemical and biochemical processes. Unfortunately, online mass spectrometry has had limited application due to high instrument costs and limited availability. Here, we detail the design, construction, and performance characteristics of a custom ion-molecule reactor retrofitted to a commonly used single quadrupole mass spectrometer to operate as an online chemical ionization mass spectrometer (CIMS). This low-cost modified CIMS is capable of limits of detection below 10 parts per trillion for select VOCs including dimethyl sulfide, dimethylamine, and trimethylamine.



INTRODUCTION

Volatile organic compounds (VOCs) are a class of organic compounds that exhibit high vapor pressure under ambient conditions. VOCs come from a wide range of biogenic and anthropogenic sources. VOC emissions have been extensively studied as they impact the environment and public health. Biogenic emissions account for the largest source of VOCs found in the atmosphere, predominantly from coniferous forests² and marine environments.³ These emissions play a major role in global atmospheric composition and climate regulation. Furthermore, VOCs also play a critical role in the formation of secondary organic aerosols (SOA), influencing their atmospheric properties and cloud-forming potential. Additionally, anthropogenic VOC emissions, including benzene, toluene, and a variety of hydrocarbons emitted from vehicle exhaust and large-scale manufacturing facilities, affect local air quality and have direct impacts on human health.^{5,6} Regulatory agencies worldwide have established guidelines and standards for VOC emissions to protect public health. However, given the vast number of VOCs and their varying toxicities, there is ongoing research to better understand their health impacts and to develop more effective control strategies.

VOCs can offer valuable information about the sources from which they originate, but due to diffusion and transport, they can exhibit spatial and temporal dependencies that complicate their detection. VOC concentrations can quickly attenuate with distance from their source and can be susceptible to degradation and other chemical reactions once emitted to the environment. For example, the atmospheric lifetimes of apinene and b-pinene are 2-3 h and around 40-80 min for limonene. Consequently, online methods for monitoring VOCs with high temporal resolution offer a major advantage compared to offline methods typically used for VOC analysis,

like gas-chromatography mass spectrometry (GC/MS) and gas-chromatography flame ionization detector (GC-FID).8 One online technique capable of real-time VOC detection is called chemical ionization mass spectrometry (CIMS).

CIMS is a sensitive and selective technique capable of continuous in situ mass analysis of volatile species.9,10 Chemical ionization allows for continuous ionization of gasphase analytes by promoting collisions with reagent ions in a controlled ion-molecule reaction (IMR) chamber. Chemical ionization is contingent on the relative chemical energetics between the reagent and the analyte, where ionization typically occurs through one of four ionization pathways: proton transfer reaction R1, adduct formation R2, charge transfer reaction R3, or proton abstraction R4.1

$$XH^+ + M \rightarrow MH^+ + X$$
 (R1)

$$X^{+} + M + Z \rightarrow MX^{+} + Z \tag{R2}$$

$$X^+ + M \to M^+ + X \tag{R3}$$

$$X^{+} + MH \rightarrow M^{+} + HX \tag{R4}$$

Unlike other mass spectrometric techniques, CIMS can strategically use a variety of reagent ions to selectively ionize specific classes of organic compounds. For example, water cluster reagent ions have been used to ionize a broad range of oxygen and nitrogen-containing compounds typically through

Received: February 18, 2024 Revised: May 15, 2024 Accepted: May 21, 2024 Published: June 14, 2024





proton transfer R1 and adduct formation R2 reaction pathways. ^{12,13} Additionally, benzene reagent ions have been employed for the ionization of sulfur-containing compounds, monoterpenes, and sesquiterpenes by charge transfer R3. ^{14,15} More recently, acetate and iodide reagent ions enable negative mode chemical ionization of organic, halo-organic, and inorganic acids, typically via proton abstraction R4. ^{16,17} This chemical selectivity provides advantages over other less targeted ionization methods by limiting spectral complexity as chemical ionization tends to retain molecular ions with minimal fragmentation.

These low-energy ionization reactions are facilitated by an ion-molecule reactor (IMR). There are a range of reaction chambers utilized in online ambient air sampling. The simplest form of reactor, of which is described in this work, consists of a multielectrode reactor which is pressure, temperature, and voltage (DC) controlled. More sophisticated reaction chambers are more complex and increase instrument costs.

To better resolve complex heterogeneous samples, both commercial and custom-built online mass spectrometers often utilize high-resolution mass analyzers, with an increasing number employing high-resolution time-of-flight (ToF) mass analyzers. ToFs have proven to be useful for online mass spectrometry due to their impressive resolving power, fast sampling rates, and simultaneous detection of a wide mass range. 19 Although lower-resolution mass analyzers, such as quadrupoles, are often still utilized for targeted analysis.

Commercial online mass spectrometry techniques take advantage of these performance characteristics, which allow them to boast impressive sensitivities (<1 parts per trillion by volume (pptv)), although these instruments suffer from high costs (>\$500,000) and limited commercial availability. Alternatively, custom-built CIMS instruments, commonly used in atmospheric sciences, are a less expensive option but can still cost upward of \$250,000 and require significant time and expertise to complete. This considerable financial commitment limits online analysis from being more widely utilized in atmospheric monitoring and other process monitoring applications.

In this study, we introduce an accessible approach to online mass spectrometry by employing a cost-effective method to conduct mass analysis of VOCs. This is achieved through the novel adaptation of a straightforward, custom-built IMR to a widely used commercial quadrupole mass spectrometer (MSQ-CIMS). This adaptation involves a secondhand Thermo MSQ, resulting in an overall expenditure of less than \$10,000, a fraction of the cost typically associated with such advanced analytical capabilities. The practical application of the MSQ-CIMS is demonstrated in three different scenarios: First, its deployment as a high throughput screening tool for the detection of dimethyl succinate; second, its utilization in measuring gas transfer velocities correlating with wind speed variations within the Scripps Ocean Atmosphere Research Simulator (SOARS) wind-wave channel; and third, its efficacy in monitoring VOC emissions from cyanobacteria cultures.

Additionally, this study takes the additional significant step toward democratizing advanced analytical techniques by providing comprehensive documentation on the design, fabrication, and assembly of the MSQ-CIMS. This detailed guidance is aimed at facilitating the replication and adoption of this system within the broader scientific community, thereby

expanding the accessibility and application of online mass spectrometry for multiple applications.

EXPERIMENTAL SECTION

MSQ. The central mass spectrometer used in this study is a Thermo Fisher MSQ, a single quadrupole mass spectrometer (QMS), first released in 2006 for atmospheric pressure ionization (API). Typically integrated with a liquid chromatography (LC) system, the MSQ was originally designed for the analysis of liquid samples. The unmodified MSQ utilizes an API source (Figure 1a), which, after sample nebulization,

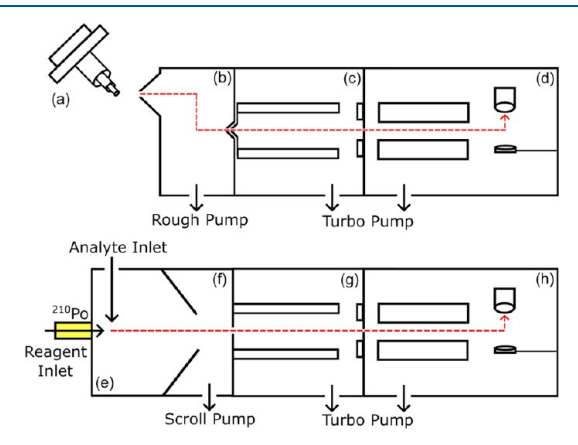


Figure 1. Diagram of the original MSQ design. (a) Original electrospray ionization probe, (b) M-path region pumped directly by the rough pump, and (c) square quadrupole transfer lens chamber with entrance cone held at 5.0 V between Sections (b) and (c). Between Sections (c) and (d), an exit aperture on the transfer lens is held at a 0.2 V potential. Region (d) consists of a quadrupole mass analyzer, conversion dynode, and electron multiplier detector; (e) and (f) are IMR electrodes 1 and 2, respectively. Section (f) is held at 20 V, externally pumped by an IDP-3 scroll pump, and interfaces directly with the square quadrupole transfer lens. Entrance cone was removed in Section (g). Sections (d) and (h) remain unchanged in the original and custom-built designs.

desolvates through a pumped intermediate "M-path" (Figure 1b) and exits through a charged cone into a square quadrupole transfer lens (Figure 1c). Ions are then transferred to a common quadrupole mass filter which detects ions via a conversion dynode coupled to an electron multiplier detector (Figure 1d). For more information about the MSQ's specification, see Supporting Information (SI).

MSQ Modifications. In Figure 1, the ESI probe (Figure 1a) and the M-path region (Figure 1b) were removed and replaced with IMR electrodes 1 and 2 (Figure 1e,f, respectively). The Thermo MSQ was modified by removing the entrance cone and interfacing the square quadrupole transfer lens directly to IMR electrode 2 (Figure 1f). IMR electrode 2 (Figure 1f) and the transfer lens chamber (Figure 1g) are interfaced with a custom spacer called the IMRinterface (see SI for details). The differential aperture on the exit of the transfer lens chamber (Figure 1g) remains unmodified and is held at a fixed 0.2 V to prevent charge build on the aperture. The mass analyzer/detector chamber of the MSQ-CIMS (Figure 1h) is identical to the Thermo MSQ (Figure 1d), and no modifications have been made to this chamber. Detailed modifications are described in the SI as well as an estimated instrument cost-break down (Table S1).

Ion-Molecule Reactor. The IMR, shown in Figure 2, consists of two aluminum electrodes which are electrically

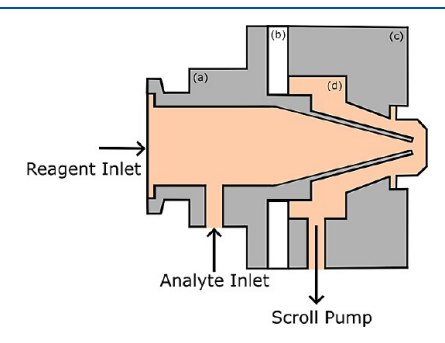


Figure 2. IMR electrode stack consists of electrode 1 (a), PTFE spacer (b), and electrode 2 (c). IMR internal volume and reaction chamber (d) are shown in orange.

isolated by a PTFE spacer. IMR electrode 1 has an internal diameter of 35.05 mm and a length of 37.85 mm and tapers down to an internal diameter of 6.30 mm. IMR electrode 2 has an internal diameter of 48.26 mm and a length of 17.27 mm and tapers to 19.03 mm (note that the IMR drawings are reported in inches). The IMR operates in the pressure range between 0.1 and 100 Torr and is regulated by a 60 L/min dry scroll pump (Agilent IDP-3). The inlet orientation shown in Figure 2 can be reversed but is not recommended due to a

decrease in linearity during calibrations (Figure S1). Further details are provided in the SI.

MSQ-CIMS Calibration and Determination of LOD. Calibrations were performed using permeation tubes purchased from VICI Metronics. Nitrogen vapor from a liquid nitrogen dewar was blown across a permeation tube using a mass flow controller (MFC). The resultant flow was then leaked into a sampling line using a low flow MFC (0-50 sccm). The sampling line was then diluted with nitrogen gas which was also controlled using an MFC (0-10 SLPM). MSQ-CIMS was operated in single ion monitoring mode (SIM). The IMR was run with 1.6 SLPM critical orifices on both the reagent and analyte inlets. The IMR was heated to 50 °C using a heating tape. All calibrations were performed under dry conditions. The pressure in the IMR was set to 40 Torr during calibrations using the benzene reagent ions, 50 Torr during calibrations using ethanol reagent ions, and 20 Torr during calibrations using water cluster reagent ions. Further details and equations for permeation tube concentrations and LOD calculations can be found in the SI.

Rapid Detection of Dimethyl Succinate. Dimethyl succinate was manually injected into a custom-built dynamic solution injection (DSI) system.²⁰ Briefly, the DSI system consists of a repurposed GC inlet which is heated to vaporize liquid samples and a carrier gas line to transfer the vaporized samples to the inlet of the MSQ-CIMS. Nitrogen vapor from a liquid nitrogen dewar was used as a carrier gas which was

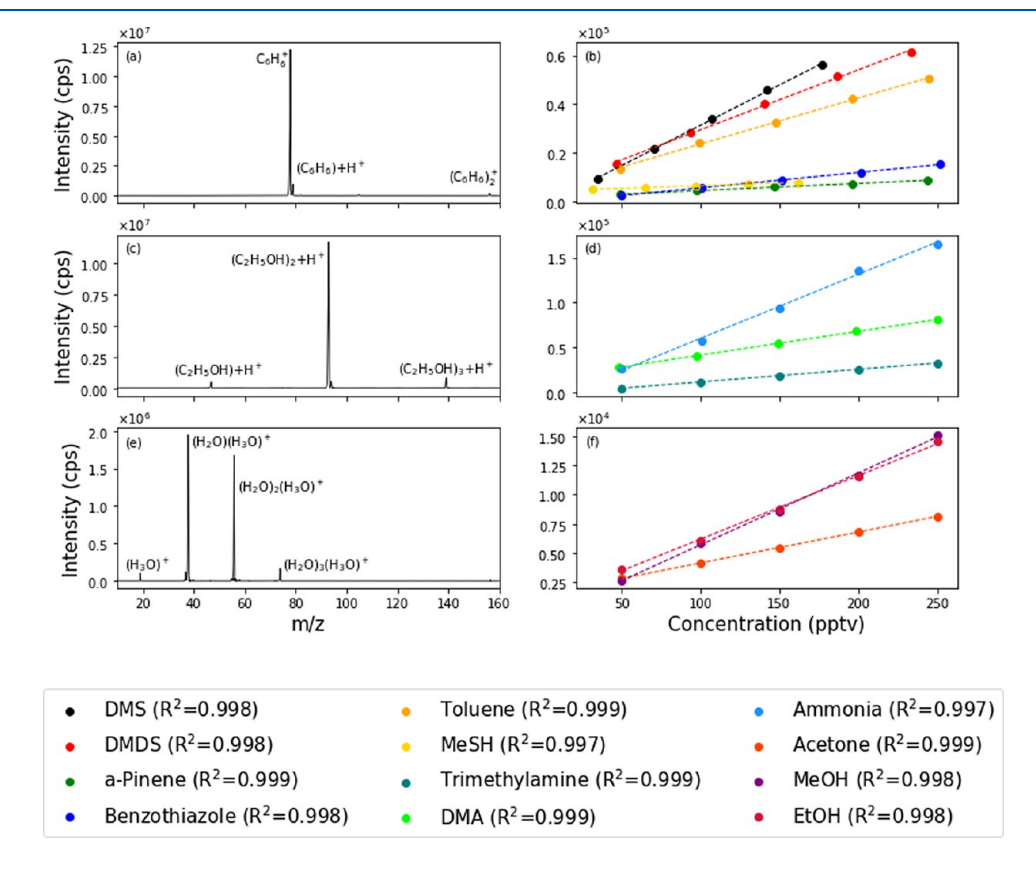


Figure 3. (a) Benzene reagent ion distribution used for the calibration of DMS, DMDS, a-pinene, benzothiazole, toluene, and MeSH. Benzene has a base peak at $78 \ m/z$ with an intensity of 1.24×10^7 cps (b) calibration curves of each calibrant detected with benzene. (c) Ethanol reagent ion distribution used for the detection and calibration of TMA, DMA, and ammonia. Ethanol has a base peak at $93 \ m/z$ with an intensity of 1.26×10^7 cps (d) calibration curves of TMA, DMA, and ammonia. (e) Ion distributions of water cluster reagent ions used for the calibration and detection of acetone, methanol, and ethanol. Water clusters have a base peak at $37 \ m/z$ with an intensity of 1.90×10^6 cps (f) calibration curves of acetone, methanol, and ethanol.

controlled by an MFC. The inlet was set to 250 $^{\circ}$ C, and samples were manually injected using a 10 uL syringe. Dimethyl succinate samples were prepared in cyclohexane at different concentrations: 5, 10, and 15 g/L.

SOARS Gas Transfer Velocity Experiment. The MSQ-CIMS was deployed in a research campaign led by the NSF Center for Aerosol Impacts on Chemistry of the Environment (CAICE) at the Scripps Ocean Atmosphere Research Simulator (SOARS) user facility at Scripps Institution of Oceanography in La Jolla, California. Newly commissioned in June 2022, SOARS is a wind-wave channel capable of simulating oceanic breaking wave conditions in a laboratory setting while controlling wind speed, aqueous chemistry, biology, air and water temperatures, and other variables. In this research campaign, the MSQ-CIMS monitored dimethyl sulfide (DMS) headspace concentrations in the SOARS windwave channel as a function of wind speed during a series of DMS gas flux experiments. During this experiment, the wave channel seawater was spiked to a final aqueous DMS concentration of 140 nM and mixed with two circulating pumps for 24 h. The headspace above the wave channel was sampled through 1/4" OD Teflon tubing at a flow rate of 1.60 SLPM. Benzene reagent ions were used to measure DMS. The MSQ-CIMS was operated at a 1 Hz sampling rate (1 Hz = 1 full scan/1s) across a mass range of m/z 55–70. Aqueous and headspace concentrations of DMS were monitored by In-Tube Extraction (ITEX)-GC-MS and MSQ-CIMS, respectively. Here, we only report the DMS headspace intensity data which are relevant to the MSQ-CIMS.

Detection of Beta-Ionone Emissions from Synecho**coccus Elongatus.** The MSQ-CIMS was used to analyze the VOC signatures of a culture of freshwater cyanobacteria, Synechococcus elongatus, over a 9 day period. The culture was grown in BG-11 growth media in a 10 L carboy. The carboy was bubbled with 2 SLPM air supplied by a zero-air generator. A vent port was added to prevent pressure build up in the carboy. The out flow at the vent was measured at 2 SLPM using a flow meter. The vent outflow was then sampled by the MSQ-CIMS at 1.6 SLPM. The IMR was operated at 40 Torr, and benzene was used as the reagent ion. The MSQ-CIMS was set to acquire between a mass range of m/z 15 and 250 at a sample rate of 0.125 Hz. Signal intensities were averaged into 1 h intervals. Molecular identification of VOC signatures emitted from Synechococcus elongatus was identified previously using GC-MS by Sauer et al.²¹ and used for annotation in this study.

■ RESULTS AND DISCUSSION

Evaluation of Reagent Ion Distributions. During inlaboratory calibration studies, reagent ion distributions of benzene largely favor the formation of the benzene cation monomer $(m/z \ 78)$ with the benzene dimer $(m/z \ 156)$ intensity being less than 1% of the monomer (Figure 3a). This reagent distribution differs from the benzene reagent distribution reported by Kim et al., where they report the benzene dimer as the primary reagent peak in their QMS. They attribute this dimer formation to the softer electric fields of their QMS system. However, in our system, the electric potential applied to the IMR electrode 2 exerts a significant effect on reagent ion declustering. Therefore, it is likely that larger benzene reagent clusters briefly exist inside our IMR but are declustered more effectively than in the design of Kim et al. 14

The ethanol reagent dimer is the molecular ion under which the IMR conditions of the calibrations shown in Figure 3c were performed. The ethanol monomer (m/z 47) and trimer (m/z 139) intensities are 2.1 and 5.8% of the ethanol dimer, respectively. This distribution is similar to the distribution reported by Yao et al.,²² where the ethanol dimer is reported to be the most abundant reagent ion, followed by the ethanol monomer and trimer.

Figure 3 shows the water cluster distribution (Figure 3e) during the calibration of acetone, methanol, and ethanol (Figure 3f). The water dimer is the molecular ion peak with the monomer, trimer, and tetramer with an abundance of 4.2, 85.4, and 8.3% of that of the dimer, respectively. Aljawhary et al. 12 report the water cluster reagent distribution in their system to be n = 3, 2, 4 listed in descending intensity where n is the number of water molecules in the cluster. Similar to Kim et al., 14 Aljawhary et al. 12 note that larger clusters likely exist in their IMR and suggest that the higher abundance of water reagent dimers is due to the fragmentation of higher order clusters. Although we are unable to directly measure the actual cluster distributions in our IMR, the cluster distribution reported here is consistent with the distribution reported by Aljawhary et al. 12

The MSQ-CIMS is theoretically capable of operating with other reagent ions not described here as well as operating in negative ion mode. Ethanol and benzene were chosen as they have been shown to selectively ionize certain classes of compounds with special selectivity and with lesser fragmentation. These reagents are also relatively cheap, have low-toxicity, and are easy to find compared to other reagents such as methyl iodide. Additionally, these reagents have low evacuation times on the internal aluminum surfaces of the IMR, whereas reagents including ammonia can have long carry over effects.

Analyte Ionization and Limits of Detection. Calibrations using benzene reagent ions were performed for select VOCs. Horning et al.²³ and Leibrock et al.²⁴ describe three ionization reaction pathways for benzene:

$$(C_6H_6)^+ + A \rightarrow (C_6H_6) + A^+$$
 (R5)

$$(C_6H_6)^+ + B \rightarrow (C_6H_5) + BH^+$$
 (R6)

$$(C_6H_6)_2^+ + X \to X^+(C_6H_6) + (C_6H_6)$$
 (R7)

R5 undergoes a direct charge transfer with the analyte where ionization is determined by relative ionization energies. Benzene has an ionization energy of 9.24 eV, and the benzene dimer has a theoretically determined ionization energy of 8.6 eV. Calibrants that were ionized via the charge transfer ionization pathway shown in Figure 3b were DMS, dimethyl disulfide (DMDS), a-pinene, benzothiazole, and toluene. The MSQ-CIMS detects methanethiol (MeSH) primarily at m/z 126, suggesting that direct adduct formation with the benzene monomer is occurring. It is unlikely to proceed through R7 in the absence of the benzene dimer, although the true reaction pathway for the ionization of MeSH in this system is unknown.

Ethanol cluster reagent ions were used for the ionization of select nitrogen-containing compounds, namely, ammonia, dimethylamine (DMA), and trimethylamine (TMA). Ethanol reagent clusters present in the reagent spectrum for the calibrations in Figure 3c were the ethanol monomer, dimer, and trimer. Ethanol reagent ionization pathways are described by Yao et al.²²:

$$(C_2H_5OH)H^+ + A \rightarrow (C_2H_5OH) + AH^+$$
 (R8)

$$(C_2H_5OH)H^+ + A + Z \rightarrow (C_2H_5OH)AH^+ + Z$$
 (R9)

DMA and TMA were detected as their nominal mass plus $\mathrm{H^+}$, indicating these species underwent a proton transfer reaction R8 with ethanol. Ammonia was detected at m/z 64, suggesting it is ionized via adduct formation with ethanol R9. Calibrants ionized by ethanol reagent ions are shown in Figure 3.

Water cluster reagent ions were used for the detection of ethanol, methanol, and acetone. The MSQ-CIMS detects all three of these calibrants as forming adducts with water. Acetone ion mass is detected at m/z 77, ethanol ion mass is detected at m/z 64, and methanol ion mass is detected at m/z 51. Water cluster chemistry is described 12 to ionize select analytes via two proposed mechanisms:

$$(H_2O)_nH^+ + A \to AH^+ + (H_2O)_n$$
 (R10)

$$(H_2O)_nH^+ + A + Z \rightarrow (H_2O)_nAH^+ + Z$$
 (R11)

R10 is direct proton transfer of analytes with proton affinities greater than that of the water clusters. Because the water reagent spectrum in this system favors the formation of the water dimer which has a proton affinity of 808 kJ/mol, it is unable to ionize methanol (PA = 754 kJ/mol) and ethanol (PA = 776 kJ/mol) by proton transfer. Instead, under these calibration conditions, methanol and ethanol are ionized by reaction pathway R11, forming adducts with water. It is worthy to note that although acetone has a proton affinity of 812 kJ/mol which is higher than the proton affinity of the water dimer, it too forms an adduct with water and is detected at m/z 77. Calibrants ionized by water cluster reagent ions are shown in Figure 3.

A summary of calibrant ionization formulas, ionization masses, and limit of detection is provided in the SI (Table S2). For all analytes, the MSQ-CIMS provides limits of detection below 40 pptv. Notably, TMA and DMA were ionized using ethanol reagent ions, resulting in LOD's calculated to be 3 and 4 pptv, respectively. DMS was the only other VOC with an LOD below 10 pptv. Calibrants detected by water cluster reagent ions overall had a higher LOD than other reagent ion calibrants (between 20 and 40 pptv). We speculate that the water cluster reagent provides higher LODs because of the lower abundance of water monomer and dimer ions as higher order water clusters do not participate in proton transfer with the analytes studied here.

It is important to note that these calibrations were performed under dry conditions. Humidity-dependent sensitivity has been shown to be analyte dependent. For example, Kim et al., in 2016, shown that DMS sensitivity is negatively correlated with increases in humidity and has a maximum sensitivity of 23 ncps/pptv at a specific humidity of 6.7 g/kg. Additionally, a-pinene sensitivity was shown to be positively correlated with specific humidity and has a maximum sensitivity of 41 ncps/pptv at a specific humidity of 11.7 g/kg.

It is shown in supplemental Figure S3 that the MSQ-CIMS sensitivity to a-pinene increases with increased humidity, whereas DMS sensitivity decreases with increased humidity. These overall trends are consistent with those reported by Kim et al., in 2016. Although humidity-dependent sensitivity is analyte specific, most analytes exhibit a loss of sensitivity as humidity increases, with rare exceptions reported for select few

VOCs including a-pinene. In the calibrations performed here, the MSQ-CIMS has a maximum sensitivity of 48 cps/pptv at a specific humidity of 0 g/kg for DMS and a maximum sensitivity of 40 cps/pptv at a specific humidity of 16 g/kg for a-pinene. Calibrations were performed in SIM mode and are unnormalized. Humidity-dependent sensitivity plot for DMS and a-pinene is presented in the SI (Figure S2).

IMR Operation and Reagent Ion Tuning. IMR tuning was performed with benzene as the reagent ion and was controlled by a 300 sccm critical orifice on the reagent inlet with the analyte inlet closed. A 300 sccm orifice was used to operate the IMR across a wider pressure range. All voltages and pressures downstream of the IMR were held constant across all pressure and voltage sweeps shown in Figure 4. IMR electrodes

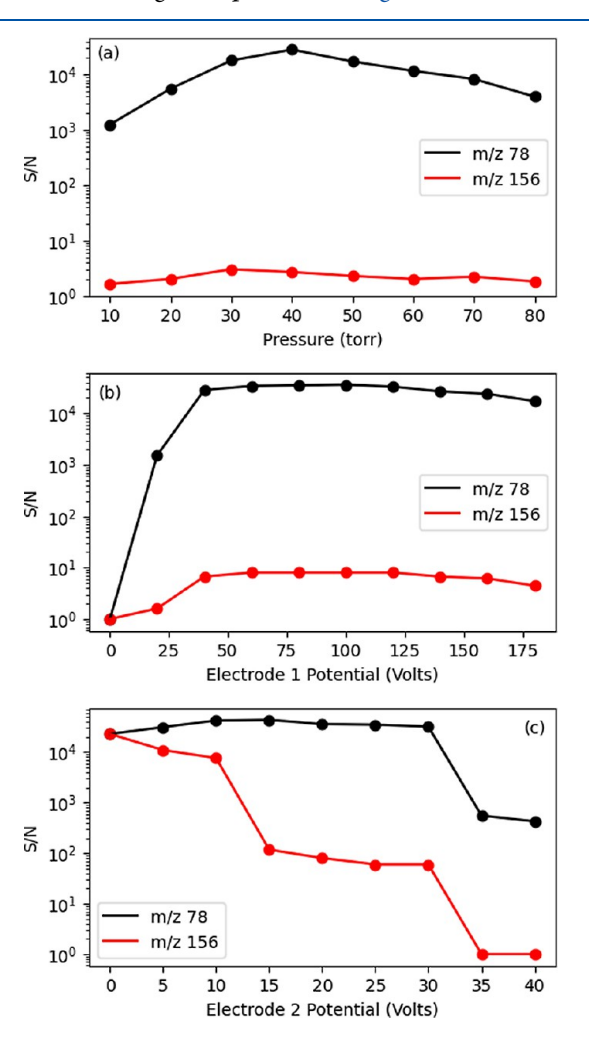


Figure 4. Benzene monomer (m/z 78) and dimer (m/z 156) signal-to-noise ratio (S/N) plotted as a function of (a) IMR pressure, (b) IMR electrode 1 voltage, and (c) IMR electrode 2 voltage.

1 and 2 were set to 50 and 20 V while scanning through pressure settings. Once the optimized pressure setting was determined, the IMR pressure was set to 40 Torr. The IMR electrode 1 voltage was then increased from 0 to 200 V by 20 V increments. IMR electrode 1 was then set to 100 V. IMR electrode 2 was then scanned through the range of 0–40 V incremented by 5 V. It was determined that the optimal IMR setting for the formation of the benzene monomer reagent was IMR operated at 40 Torr (Figure 4a), IMR electrode 1 set to 100 V (Figure 4b), and IMR electrode 2 set to 15 V (Figure

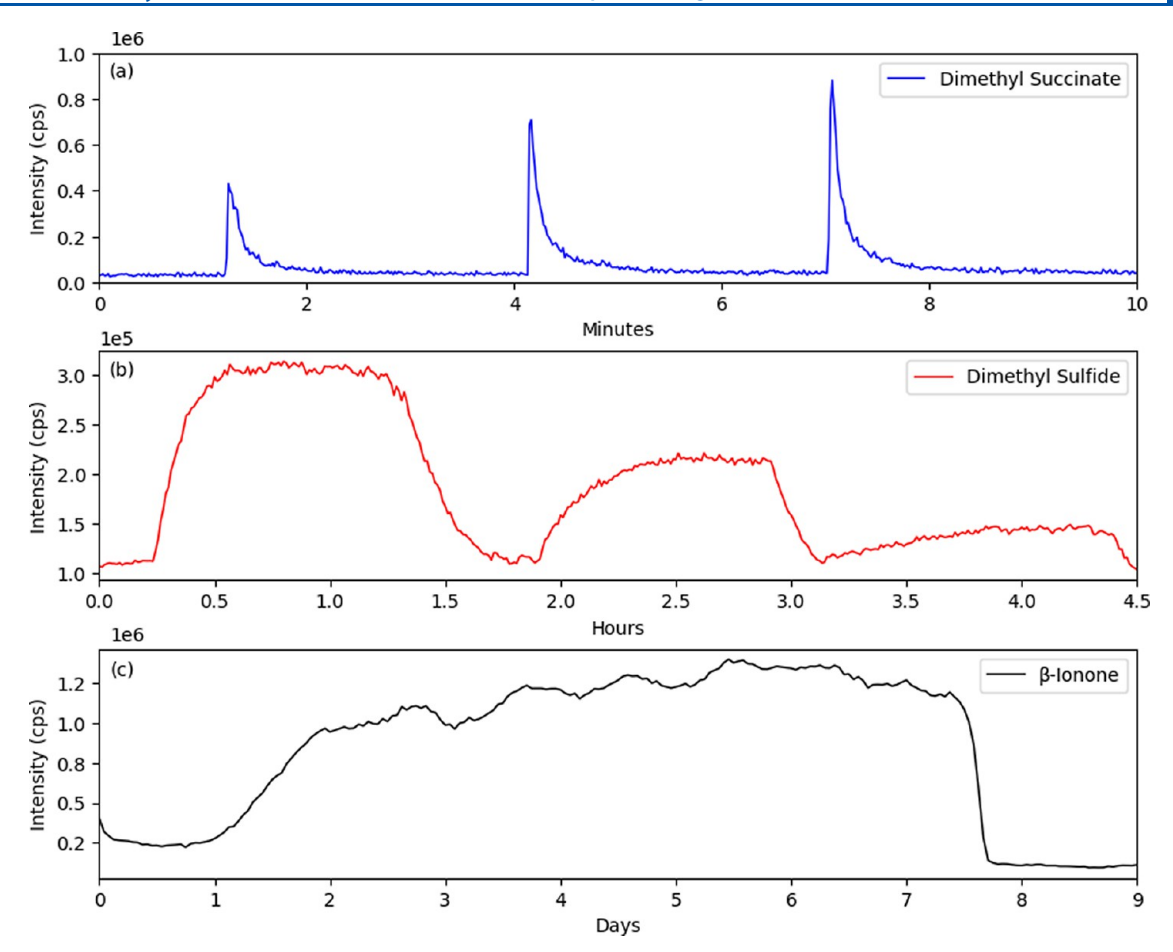


Figure 5. (a) Time series plot of dimethyl succinate DSI across 3 different sample concentrations over a 10 min sampling period. 5, 10, and 15 g/L samples were injected at 1, 4, and 7 min postexperiment start time, respectively. (b) Time series plot of dimethyl sulfide headspace intensities in the SOARS wind and wave channel at 3 different wind speeds across the 4.5 h experiment. 15.2, 9.7, and 4.2 m/s wind speeds were started at 0.2, 1.8, and 3.1 h, respectively. (c) Time series plot of the headspace concentration of beta-ionone produced during the growth and death cycle of *S. elongatus* over 9 days.

4c). Other combinations of IMR settings were tested, but only select combinations are presented here. There may exist other conditions that are preferential to the conditions shown in Figure 4.

IMR electrode 1 voltage must exceed the voltage of electrode 2 to ensure a "downhill" potential and allow ions to be directed through the IMR. Pressure control is critical to optimizing the S/N ratio of the reagent ion and should be operated between 10 and 100 Torr, depending on the reagent ion. Finally, IMR electrode 2 voltage is mainly responsible for controlling the cluster distributions of each reagent ion. Experimentally, we notice fragmentation of the benzene reagent ion when IMR electrode 2 is set above 30 V (Figure 4). IMR optimization was also performed for both ethanol and water reagent ions and included in the SI (Figures S3 and S4). It is important to note that reagent ion signal is not directly proportional to analyte sensitivity. Specific reagent ion distributions may be better suited for specific analytes. Furthermore, different analyte-reagent combinations can have unique IMR conditions which optimize analyte detection. Figures 4, S3, and S4 are included to provide a reference for how to effectively operate the IMR for each reagent ion and show how the voltage and pressure settings effect overall signal.

Rapid Detection of Dimethyl Succinate. Figure 5a shows a time series plot of intensities of dimethyl succinate injected into a heated DSI manifold (see methods Section 2.4).

As subsequent samples were injected into the DSI, they were vaporized by the heated inlet and detected with the MSQ-CIMS. Three samples were injected into the manifold across a 10 min period with increasing concentrations (5, 10, and 15 g/L). The fast sampling rate of the MSQ-CIMS allows for rapid detection and quantification of transient signals in real time. These measurements using the DSI manifold greatly expand the capabilities of the MSQ-CIMS to ionize both liquid and gas samples. Furthermore, the rapid clearance time of the IMR (around 1 min) makes it possible to perform high throughput screening of liquid samples. For the detection of dimethyl succinate, at a 2 min sampling rate, the MSQ-CIMS can quantify samples 10× faster than current HPLC methods. 26

SOARS Gas Transfer Velocity Experiment. The headspace intensity of DMS in the SOARS wave channel during the gas transfer velocity measurements made during the 2022 summer research campaign is shown in Figure 5b. The MSQ-CIMS detected changes in headspace intensities of DMS as the wind speed inside the channel was stepped down from high to medium to low wind speeds (15.2, 9.7, and 4.2 m/s, respectively). High, medium, and low wind speeds were started at 0.2, 1.8, and 3.1 h, respectively (Figure 5b). Each wind speed was followed by a decay period where the winds were turned off and the DMS intensity was allowed to decay back to baseline. The MSQ-CIMS can provide useful mass

spectral data while preserving information about how spectral intensities change over time with varying conditions.

Detection of Beta-Ionone Emissions from Synechococcus Elongatus. For the carboy study shown in Figure 5c, beta-ionone emitted from S. elongatus was monitored across the growth and death phases of the culture. The culture was grown for 6 days uninterrupted, and on day 6, intentionally contaminated with a heterotrophic bacteria grazer. The MSQ-CIMS was used to monitor the headspace of a wide range of masses, but only the time series of beta-ionone is shown in Figure 5c. The MSQ-CIMS ran continuously for 9 days across the experiment with only minor breaks to clear sampling lines of condensed water droplets. This experiment provides an important case study for the MSQ-CIMS for realtime monitoring of processes. A major advantage of real-time MS is the ability to operate for long periods of time to capture temporal and spatial trends. This performance characteristic is critical to be maintained in any new real-time MS build. The experiment was run for 9 days and only ended because the culture had crashed, triggering the completion of the experiment. Theoretically, the MSQ-CIMS could be run for much longer, although we are yet to test its ability to run for greater than 1 month. Other CIMS instruments can run continuously for multiple months which suggests that this is also feasible for the MSQ-CIMS.

CONCLUSIONS

The fabrication of the MSQ-CIMS highlights three important points about the state of online mass spectrometry:

- 1. There is a lack of publicly available information detailing and characterizing custom-built IMRs. Descriptions and block diagrams of IMRs exist in the literature, but we are unaware of any publications that include CAD drawings and assembly instructions that are readily available to the public. This study provides details on building a low-cost CIMS, as well as detailing a simple yet robust IMR system.
- 2. These modifications are not limited to application on single quadrupole systems. The Thermo MSQ is a legacy instrument that can be purchased for low cost on secondary markets, but theoretically, other benchtop LC/MS systems should be capable of operating in this manner. Although quadrupoles have lower resolving power than modern ToFs, for most targeted analysis applications, they provide ample resolution and scanning speeds while keeping instrument cost low. More modern systems could offer lower limits of detection as well as tandem MS capabilities which would aid in identifying VOC precursor ions. It is shown here that commercial systems are capable of operating in an "online mode" which can greatly expand their utility. Commercial GC/ MS instruments were considered for this build, but an LC/MS system was preferred because of the integrated vacuum system designed to interface with atmospheric pressure. GC/MS systems can theoretically be retrofitted for online analysis, but sample introduction and pressure regulation would be additional important considerations.
- 3. The low cost of the MSQ-CIMS can greatly expand the adoption of online gas analysis as a common technique in a variety of sectors. For example, similar to the application shown in Figure 5c, online VOC analysis was

shown by Sauer et al., in 2021, as a rapid method for determining biological contamination in commercially grown cyanobacteria cultures. However, adoption of this technique for quality control analysis by the greater algae cultivation community is slowed by large instrument costs. Not only does the MSQ-CIMS have potential to resolve this issue by providing growers with an inexpensive tool for rapid quality control analysis but it can also facilitate further investigation into online mass spectrometry as a method for process monitoring more broadly, including in the agriculture and fermentation industries. Additionally, for current users of online mass spectrometers, a low-cost instrument makes it more feasible to deploy multiple instruments for a single application. This can be especially useful for VOCs with high-spatial dependencies or when monitoring VOC emissions across a given area. Running multiple reagent ion chemistries in tandem can help broaden the detection capabilities without delays or complexities imparted by reagent ion switching mechanisms. Overall, we hope that the thorough dissemination of this ion source modification will stimulate the community to adopt, improve, and share their own IMR designs for implementation on other commercial low-cost or legacy MS instrumentation.

ASSOCIATED CONTENT

Supporting Information

The Supporting Information is available free of charge at https://pubs.acs.org/doi/10.1021/acs.analchem.4c00916.

Additional MSQ modification, IMR, and calibration details and IMR drawings as well as photographs of IMR assembly with instructions (PDF)

AUTHOR INFORMATION

Corresponding Author

Kimberly A. Prather – Department of Chemistry and Biochemistry, University of California, San Diego, California 92093, United States; Scripps Institution of Oceanography, University of California San Diego, La Jolla, California 92093, United States; Email: kprather@ucsd.edu

Authors

Benjamin Rico — Department of Chemistry and Biochemistry, University of California, San Diego, California 92093, United States; © orcid.org/0009-0007-0024-8806

Jon S. Sauer — Department of Chemistry and Biochemistry, University of California, San Diego, California 92093, United States; orcid.org/0000-0001-7527-109X

Robert S. Pomeroy — Department of Chemistry and Biochemistry, University of California, San Diego, California 92093, United States; orcid.org/0000-0002-9787-1050

Complete contact information is available at: https://pubs.acs.org/10.1021/acs.analchem.4c00916

Note:

The authors declare no competing financial interest.

ACKNOWLEDGMENTS

This work was supported by the National Science Foundation (NSF) Center for Aerosol Impacts on Chemistry of the Environment (CAICE) Grant (Award number: CHE-

1801971). Any opinions, findings, and conclusions or recommendations expressed in this material are those of the author(s) and do not necessarily reflect the views of the NSF. The authors thank Berk Kuntasal for preparation of dimethyl succinate samples and Ryan Simkovsky for preparation of S. Elongatus cultures. We also thank Joe Mayer for his help machining IMR components.

REFERENCES

- (1) David, E.; Niculescu, V. C. Int. J. Environ. Res. Public Health **2021**, 18 (24), No. 13147.
- (2) Antonelli, M.; Donelli, D.; Barbieri, G.; Valussi, M.; Maggini, V.; Firenzuoli, F. Int. J. Environ. Res. Public Health 2020, 17 (18), No. 6506.
- (3) Zhao, D.; Yang, Y.; Tham, Y. J.; Zou, S. Mar. Environ. Res. 2023, 191, No. 106177.
- (4) Mayer, K. J.; Wang, X.; Santander, M. V.; Mitts, B. A.; Sauer, J. S.; Sultana, C. M.; Cappa, C. D.; Prather, K. A. ACS Cent. Sci. 2020, 6, 2259–2266.
- (5) Montero-Montoya, R.; López-Vargas, R.; Arellano-Aguilar, O. Ann. Global Health 2018, 84 (2), 225–238.
- (6) Soni, V.; Singh, P.; Shree, V.; Goel, V. Effects of VOCs on Human Health. In Sharma, N.; Agarwal, A.; Eastwood, P.; Gupta, T.; Singh, A., Eds.; Air Pollution and Control. Energy, Environment, and Sustainability; Springer: Singapore, 2018.
- (7) Kesselmeier, J.; Staudt, M. Journal of Atmospheric Chemistry 1999, 33, 23-88.
- (8) Perraud, V.; Meinardi, S.; Blake, D. R.; Finlayson-Pitts, B. J. Atmos. Meas. Technol. 2016, 9, 1325–1340.
- (9) de Gouw, J.; Warneke, C. Mass Spectrom. Rev. 2007, 26, 223-257.
- (10) Huey, L. G. Mass Spectrom. Rev. 2007, 26, 166-184.
- (11) Munson, B. Encycl. Anal. Chem. 2000, 1-22.
- (12) Aljawhary, D.; Lee, A. K. Y.; Abbatt, J. P. D. Atmos. Meas. Technol. 2013, 6, 3211-3224.
- (13) Pfeifer, J.; Simon, M.; Heinritzi, M.; Piel, F.; Weitz, L.; Wang, D.; Granzin, M.; Müller, T.; Bräkling, S.; Kirkby, J.; Curtius, J.; Kürten, A. Atmos. Meas. Technol. 2020, 13, 2501–2522.
- (14) Kim, M. J.; Zoerb, M. C.; Campbell, N. R.; Zimmermann, K. J.; Blomquist, B. W.; Huebert, B. J.; Bertram, T. H. Atmos. Meas. Technol. **2016**, *9*, 1473–1484.
- (15) Lavi, A.; Vermeuel, M. P.; Novak, G. A.; Bertram, T. H. Atmos. Meas. Technol. 2018, 11, 3251–3262.
- (16) Brophy, P.; Farmer, D. K. Atmos. Meas. Technol. 2016, 9, 3969—
- (17) Robinson, M. A.; Neuman, J. A.; Huey, L. G.; Roberts, J. M.; Brown, S. S.; Veres, P. R. Atmos. Meas. Technol. 2022, 15, 4295–4305.
- (18) Ellis, A. M., C. A. M. Experimental: Components and Principles. In *Proton Transfer Reaction Mass Spectrometry Principles and Applications*; John Wiley & Sons, 2014; pp 50–106.
- (19) Breitenlechner, M.; Novak, G. A.; Neuman, J. A.; Rollins, A. W.; Veres, P. R. Atmos. Meas. Technol. 2022, 15, 1159–1169.
- (20) Jardine, K. J.; Henderson, W. M.; Huxman, T. E.; Abrell, L. Atmos. Meas. Technol. 2010, 3, 1569-1576.
- (21) Sauer, J. S.; Simkovsky, R.; Moore, A. N.; Camarda, L.; Sherman, S. L.; Prather, K. A.; Pomeroy, R. S. *Proc. Natl. Acad. Sci. U.S.A.* **2021**, *118* (40), No. e2106882118.
- (22) Yao, L.; Wang, M.-Y.; Wang, X.-K.; Liu, Y.-J.; Chen, H.-F.; Zheng, J.; Nie, W.; Ding, A.-J.; Geng, F.-H.; Wang, D.-F.; Chen, J.-M.; Worsnop, D. R.; Wang, L. Atmos. Chem. Phys. **2016**, *16*, 14527–14543.
- (23) Horning, E. C.; Horning, M. G.; Carroll, D. I.; Dzidic, I.; Stillwell, R. N. Anal. Chem. 1973, 45, 936–943.
- (24) Leibrock, E.; Huey, L. G. Geophys. Res. Lett. 2000, 27, 1719–1722.
- (25) Grover, J.; Walters, E.; Hui, E. J. Phys. Chem. 1987, 91, 3233–3237.

(26) Treece, T. R.; Tessman, M.; Pomeroy, R. S.; Mayfield, S. P.; Simkovsky, R.; Atsumi, S. *Metabolic Engineering* **2023**, *79*, 118–129.